Vol. 47, No. 4 (2025) 792-805, DOI: 10.24874/ti.2015.09.25.11

Tribology in Industry

www.tribology.rs

RESEARCH

Machinability of Normalized and Stress-Relieved C45 Steel in Dry Internal Turning

Henrique Oliveira Santos[a], Mickaela Ramos Barbosa[b], Carlos Eduardo dos Santos[b], Marcello Rosa Dumont[a,*]

[a]*Materials Engineering Graduate Program, Federal Center for Technological Education of Minas Gerais, Belo Horizonte, Brazil,*
[b]*Materials Engineering Department, Federal Center for Technological Education of Minas Gerais, Belo Horizonte, Brazil.*

Keywords:

C45 Steel
Dry internal turning
Chip formation
Cutting insert
Roughness
Cutting speed
Feed rate

* Corresponding author:

Marcello Rosa Dumont
E-mail: marcellodumont@cefetmg.br

Received: 4 September 2025
Revised: 8 October 2025
Accepted: 10 November 2025

ABSTRACT

This experimental study provides new insights into the dry internal turning behaviour of seamless cold-drawn DIN C45 steel tubes subjected to different heat treatment conditions (normalized and stress-relieved). Unlike conventional studies that focus solely on parameter optimization, this work emphasizes the interaction between cutting parameters and heat treatment on surface integrity and chip morphology. A factorial experimental design was applied to evaluate the combined effects of cutting speed and feed rate on surface roughness parameters arithmetic mean deviation (R_a), total profile height (R_t), and maximum profile height (R_z) while maintaining a constant cutting depth. The results highlight that feed rate and its interaction with cutting speed significantly affect surface roughness ($p < 0.05$), with normalized steel showing superior chip fragmentation and surface finish compared to the stress-relieved condition. The findings contribute to a better understanding of dry machining behaviour in medium-carbon steels, offering experimentally validated guidelines for selecting cutting parameters that improve surface quality and process efficiency while minimizing empirical testing in industrial applications.

1. INTRODUCTION

DIN C45 steel is a medium-carbon steel widely employed in engineering applications due to its combination of mechanical strength, hardness, availability, and cost-effectiveness [1,2]. Cold-drawn seamless tubes of DIN C45, when subjected to thermal treatments such as normalization or stress relief, exhibit improved dimensional stability, reduced residual stresses, and enhanced machinability, enabling the production of high-strength components including gears, pins, bushings, automotive parts, and machine elements [2,3].

Dry turning, in particular, has gained interest for reducing cutting fluids, energy consumption, and operational costs, while achieving high-quality surface finishes [4–9]. However, achieving these advantages requires careful selection of cutting parameters, including feed rate, cutting speed, and cutting depth, as well as appropriate tool geometry and coating [10-13]. Previous studies have demonstrated that feed rate and cutting speed largely govern surface roughness, while cutting depth typically has a minor influence. Biasibetti [14] and Keblouti [15] highlight that tool material and cutting conditions significantly affect chip formation and surface integrity, yet most studies focus on external turning or bar geometries rather than internal turning of tubular components.

Despite extensive research on steel machinability, limited attention has been given to internal dry turning of cold-drawn DIN C45 tubes, particularly evaluating the effects of thermal treatments on surface roughness and chip morphology. This study addresses this gap by assessing the influence of feed rate (f_r) and cutting speed (C_s) on surface roughness parameters (R_a, R_t, R_z) and chip formation in dry internal turning of normalized and stress-relieved DIN C45 tubes.

The study highlights the relevance of this choice by demonstrating the potential competitiveness of the selected material compared to traditional applications, adding value by combining scientific rigor with industrial applicability, and generating technical knowledge useful for the rational selection of cutting parameters in relation to the material's thermal conditions, with direct benefits in performance, cost, and production efficiency.

2. MATERIALS AND METHODS

The material used in all tests was DIN C45 steel, subjected to two distinct types of heat treatment: normalizing (+N), performed at 920 °C for 60 minutes, and stress relief (+SR), performed at 580 °C for 30 minutes. The chemical composition, analysed using the Thermo Fisher ARL4460 optical emission spectrometer, can be found in Table 1. The permissible values for each element according to the EN10083-2 [16] standard are also shown.

The dimensions of the test specimens used were 82.5 mm x 18 mm (external diameter x thickness) for the steel with normalizing thermal treatment (+N) and 52 mm x 7 mm (external diameter x thickness) for the steel with stress relief thermal treatment (+SR), both with an initial length of 150 mm. The experimental procedure was conducted using dry turning tests on the internal diameter surface of the test specimens. This evaluation was performed by analysing the roughness of the machined surface and the machining chips' morphology. A 3^2 full factorial design was used, with three levels and two factors, resulting in nine trials, without replicates. The independent variables (factors) were the feed rate and cutting speed, with the following levels: 0.15 mm.rev^{-1} (-1), 0.23 mm.rev^{-1} (0), and 0.30 mm.rev^{-1} (+1) for feed rate; 180 m.min^{-1} (-1), 278 m.min^{-1} (0), and 300 m.min^{-1} (+1) for cutting speed. The level values encompass the limits specified by the cutting tool manufacturers and are commonly applied in the industry.

Table 1. Chemical Composition (% by mass) of C45 Steel.

Elements	C	Si	Mn	P	S	Cr	Mo	Ni	Cr + Mo + Ni
EN10083-2 Standard	min/max 0.42/0.50	max. 0.40	min/max 0.50/0.80	max. 0.045	max. 0.045	max. 0.40	max. 0.10	max. 0.40	max. 0.63
Stress relief	0.471	0.21	0.80	0.011	0.0082	0.17	0.018	0.03	0.22
Normalized	0.461	0.22	0.68	0.009	0.0124	0.07	0.028	0.03	0.13

The machining length was kept constant at 55 mm, and the cutting depth (C_p) remained constant at 0.80 mm at the radius for each machining pass. The response variables obtained from the experiment were the R_a, R_t and R_z roughness parameters. R_a determines the average of all peaks and valleys measured along the analysis, R_t is defined as the vertical distance between the highest peak and the lowest valley, and R_z is more sensitive to occasional high peaks or deep valleys than R_a [17,18]. Table 2 presents the design of the dry turning experiments.

Table 2. Experimental Design for Stress Relief and Normalized C45 Steel.

Test	f_r	C_s
1	-1 (0.15)	-1 (180)
2	-1 (0.15)	0 (278)
3	-1 (0.15)	+1 (300)
4	0 (0.23)	-1 (180)
5	0 (0.23)	0 (278)
6	0 (0.23)	+1 (300)
7	+1 (0.30)	-1 (180)
8	+1 (0.30)	0 (278)
9	+1 (0.30)	+1 (300)

The metallographic analysis was performed on samples with a face area of 1 cm^2 (1 cm wide x 1 cm long). The samples were embedded using hot-curing phenolic resin (bakelite) at approximately 150 °C, using the PRE 30Mi Arotec metallographic embedding machine. After embedding, the sample surfaces were prepared following consecutive sanding steps, using water-resistant sandpapers with grit sizes of 120, 240, 320, 400, and 600 mesh. Afterward, they were polished in the presented sequence, using diamond paste with grit sizes of 9 µm, 3 µm, and 1 µm. The samples were etched with a 5% Nital solution to reveal the microstructure.

The hardness was determined using a Vickers microhardness tester, Shimadzu, HMV-2TE, with a 40x magnification, diamond-tipped indenter, 15 seconds penetration time and an applied load of 1961 N. Ten measurements were taken on the surface of the samples.

The tensile test was conducted using an Instron universal testing machine, model 5992, with the Blue Hill3 data acquisition system and a mechanical extensometer. The test specimens were prepared according to the requirements defined by ASTM A370 [19].

The machinability test was conducted on a Romi Centur 30D lathe, using power of 9 kW and a maximum speed of 4000 rpm. The lathe is equipped with a Siemens 810 Computer Numerical Control (CNC) software. A carbide cutting insert (Mitsubishi Materials, VBMT 110304–MV UE6020, ISO P20 class), coated with titanium nitride (TiN), was used with the FSVUB20 16R-11S tool holder. Both components were new at the start of testing. The MV model features dual chip breakers and rounded points on the cutting face. Its dimensions are shown in Fig. 1.

The R_a, R_t and R_z measurement was conducted using a contact method, with a Tesa portable roughness meter, model Rugo Surf 20, at three equidistant points horizontally across the internal surface of the test specimens. The roughness meter was configured with five cut-offs of 0.80 mm sampling length, totalling 4 mm as the total measurement length. The chips formed during the tests were analysed using a digital microscope, and their characteristics were compared with the chip classification according to the NBR ISO 3685 standard [20]. Descriptive statistical analysis of the roughness parameters was performed using the arithmetic mean, standard deviation, coefficient of variation, and variation index. Inferential statistical analysis was conducted to evaluate the influence of cutting parameters on R_a, R_t and R_z roughness using the analysis of variance (ANOVA) method with a 95 % significance level [21-24].

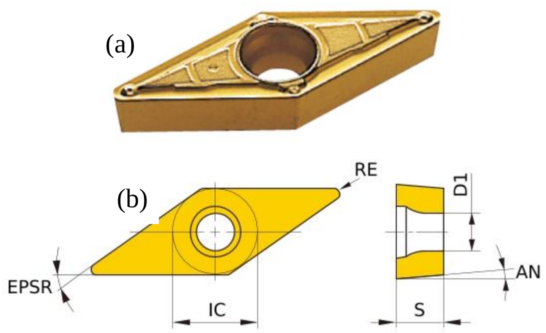

D1 - Hole diameter for mounting: 2.90 mm
IC - Diameter of the inscribed circle: 6.35 mm
EPSR - Point angle: 35°
AN - Clearance angle: 5°
S - Cutting insert thickness: 3.18 mm
RE - Point radius: 0.0 mm

Fig. 1. Cutting Insert: (a) VBMT 110304 – MV UE6020; (b) representation of cutting insert with its respective dimensions.

3. RESULTS AND DISCUSSION

The materials under consideration in this study were characterized in terms of their microstructure, hardness, and the influence of dry machining parameters on surface finish.

3.1. Metallographic analysis

The material was characterized as a hypoeutectoid steel with a microstructure consisting of ferrite (light areas) and pearlite (dark areas) [25] in both types of thermal treatments, as illustrated in Fig. 2 (a) for normalized steel and Fig. 2 (b) for stress-relieved steel. The metallographic analysis reveals that the C45 steel microstructure is consistent with the thermal treatments applied. The presence of ferrite phase is observed in light areas, while pearlite phase is present in dark areas. The main difference observed when comparing the micrographs of samples subjected to different thermal treatments is that the pearlite density in the stress-relieved sample appears to be higher compared to the normalized sample [26].

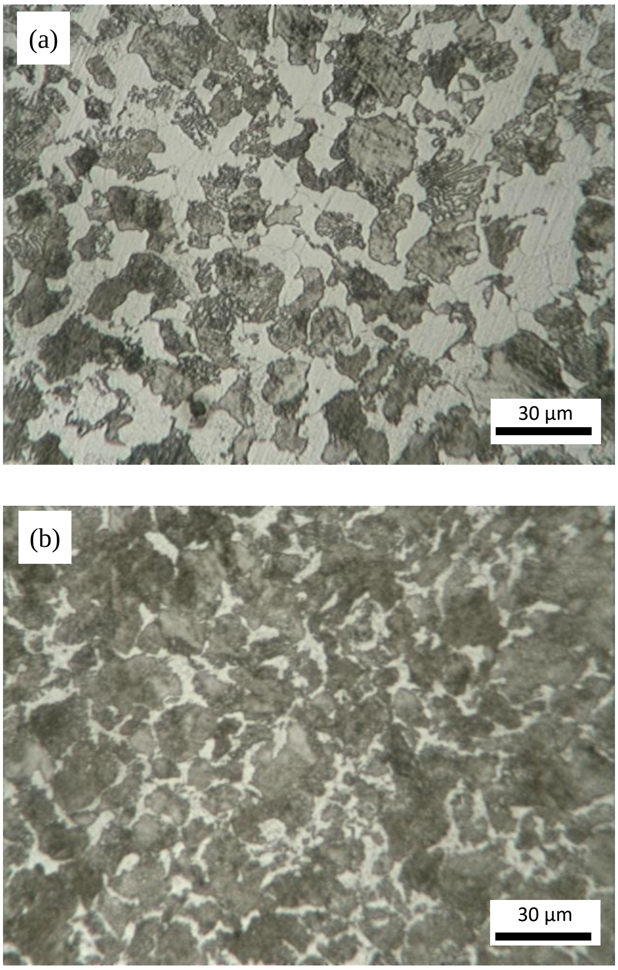

Fig. 2. Microstructure of C45 Steel with Thermal Treatments: (a) Normalized, (b) Stress Relieved.

3.2. Hardness and tensile strength

Table 3 presents the average hardness values obtained with their respective standard deviations. A hardness of 297 HV ± 13 HV was found for the stress-relieved material, where there were a higher fraction of pearlite (Fig. 2) and a hardness of 190 HV ± 7 HV for the normalized material. It can be observed that the thermal treatment has a significant impact on the hardness of C45 steel, resulting in greater hardness for the stress-relieved sample compared to the normalized one. This mechanism is explained by Bhadeshia [26], where it may arise from differences in the thermal history: normalizing via heating above the A3 temperature tends to homogenize the microstructure and frequently refine the pearlite, whereas stress-relieving undertaken at temperatures below A1 preserves the pre-existing microstructure and only modifies the defect energy state and micrographic contrast.

Table 3. Vickers Hardness of the Samples.

Treatment	Hardness (HV)
+N	190 ± 7
+SR	297 ± 13

Table 4 shows the results obtained from the tensile tests until the fracturing of the test specimens. These results represent the simple arithmetic means of tests conducted on three specimens for each type of thermal treatment and are consistent with normalized C45 steel and stress-relieved C45 steel. The results indicate that the final tensile strength is lower in the normalized state compared to the stress-relieved state. This can be attributed to the relief of internal stress during thermal treatment. However, the reduction in final tensile strength is offset by the increase in material ductility, as observed by Samir and Thapa [27].

Table 4. Mechanical Properties of C45 Steel Obtained from Tensile Testing.

Treatment	Yield strength (MPa)	Tensile strength (MPa)	Elongation (%)
+N	377 ± 9	632 ± 9	26 ± 2
+SR	461 ± 51	951 ± 27	20 ± 1

3.3. ANOVA analysis for experiments with stress-relieved C45 steel

Fig. 3 shows that all three independent variables showed significant absolute effects on all dependent variables, exceeding the minimum significance threshold of 1.975.

When evaluating the impact of the observations on the model, the feed rate variable was the most influential on all dependent variables—R_a, R_t and R_z —followed by the interaction between the cutting speed and feed rate, and finally, by the cutting speed. This behaviour is expected, as described by Arbizu and Perez [28], Barzani [23], and Kumar and Chauran [29], who state that the feed rate is generally the independent variable that most influences the surface roughness of turned parts. Similar results were observed in studies conducted by Biasibetti [14] and Filho [30].

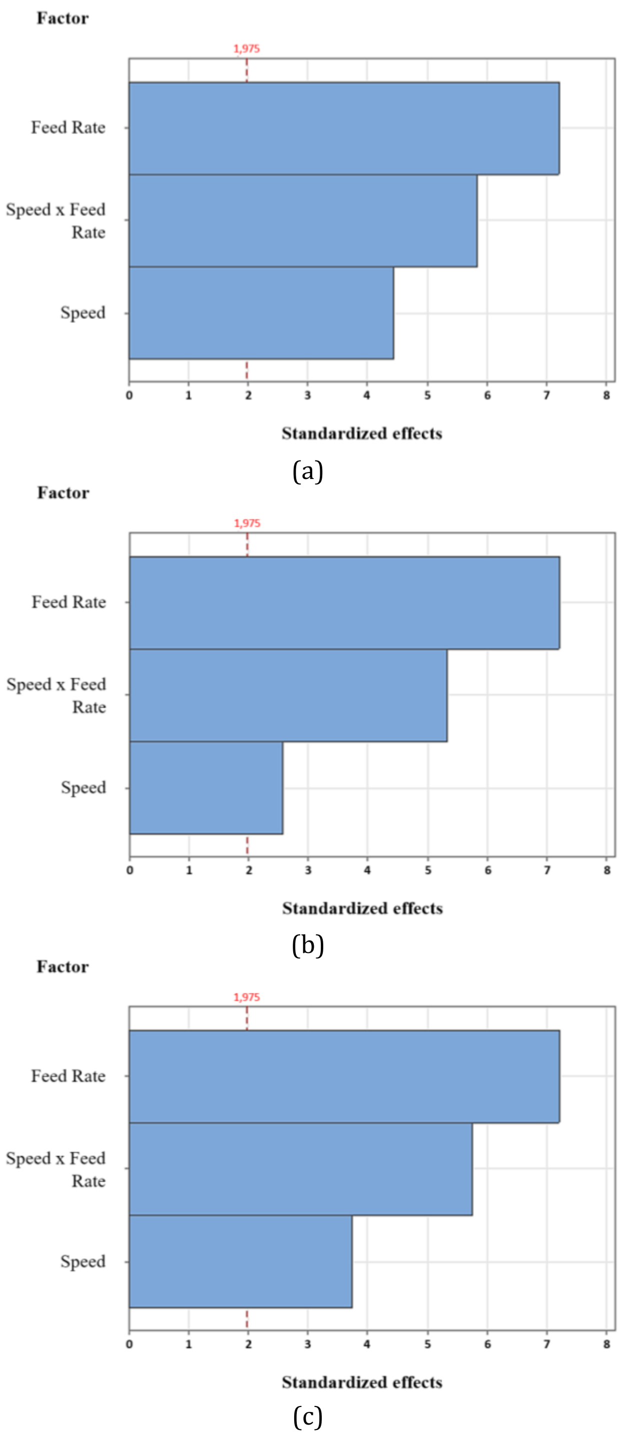

Fig. 3. Pareto Charts showing Standardized Effects of the Parameters for C45 +SR Samples, α = 0.05. (a) R_a, (b) R_t and (c) R_z.

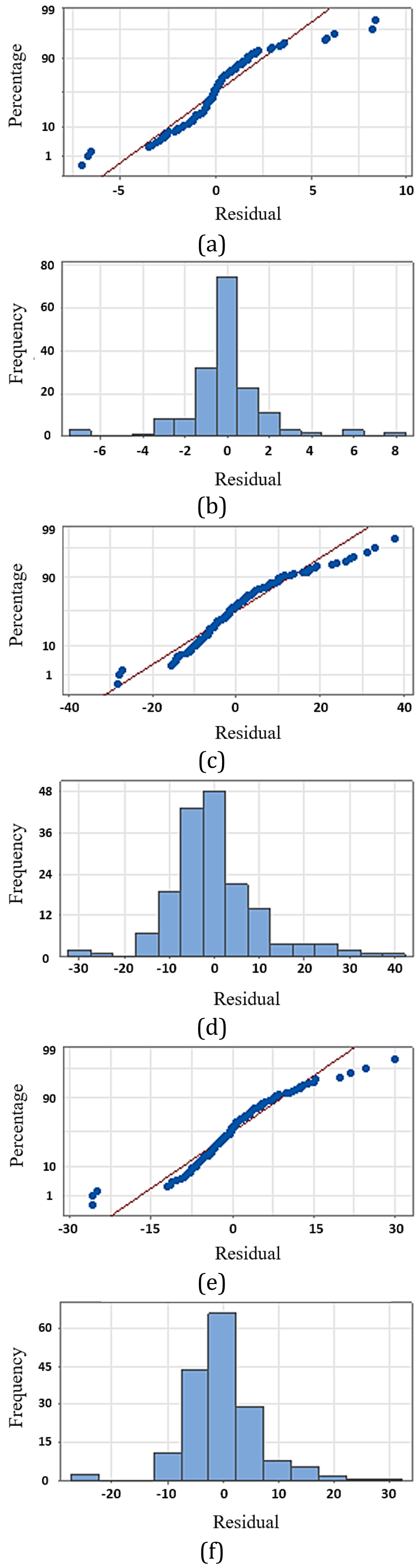

Fig. 4. Residual Plots of Parameters for C45 +SR Samples: (a) R_a normal probability, (b) R_a histogram, (c) R_t normal probability, (d) R_t histogram, (e) R_z normal probability and (f) R_z histogram.

In Fig. 4, the residual plot for the R_a, R_t and R_z roughness parameters shows that the residuals approximate a normal distribution, as indicated by the closeness of the points to the line with few outliers in the normal probability plot. The histogram of the residuals reveals an approach to normality, demonstrating data close to symmetry. These observations are consistent with the statistical assumptions discussed by Walpole [31], where residuals following an approximately normal distribution and symmetric histogram indicate the adequacy of the fitted model and the reliability of the variance assumptions used in the analysis.

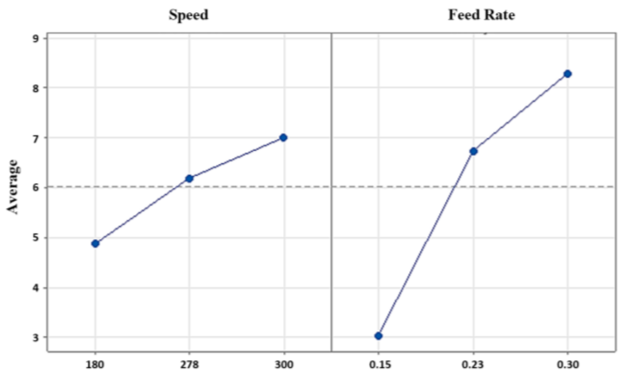

(a)

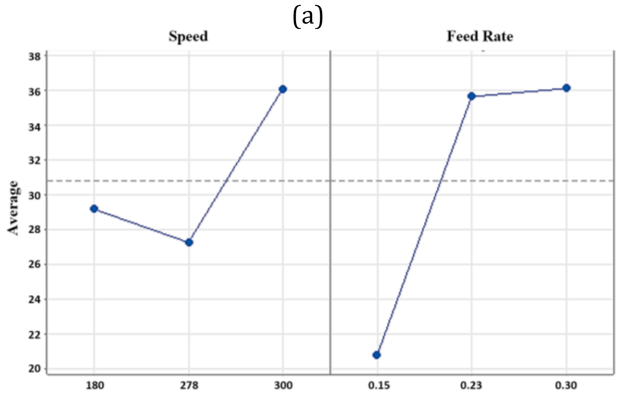

(b)

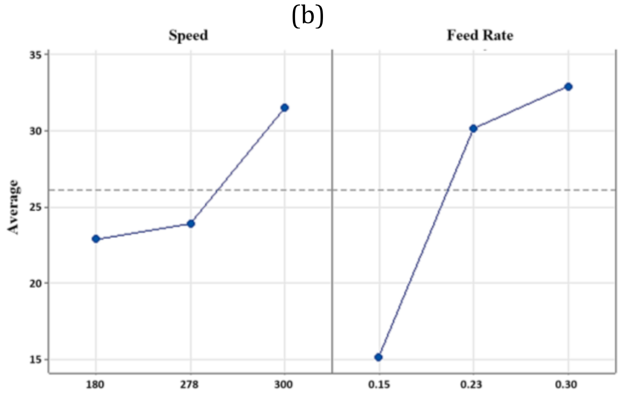

(c)

Fig. 5. Main effects plots of parameters for C45 +SR samples. (a) R_a, (b) R_t and (c) R_z.

Fig. 5 presents the main effects plot for the R_a, R_t and R_z roughness parameters. For R_a, can be observed that transitioning from a feed rate of 0.15 mm.rev^{-1} to 0.23 mm.rev^{-1} results in a significant change in the analysis, while the effect of the cutting speed increases similarly across the three factors. For the R_t parameter, there is a distinct effect with the cutting speed compared to R_a. An inflection in the cutting speed variable can be clearly seen, indicating a decrease in roughness when moving from 180 m.min^{-1} to 278 m.min^{-1} and an increase when moving from 278 m.min^{-1} to 300 m.min^{-1}. However, concerning the feed rate, the same pattern identified in R_a is observed, where the transition from 0.15 mm.rev^{-1} to 0.23 mm.rev^{-1} results in a significant change in R_t.

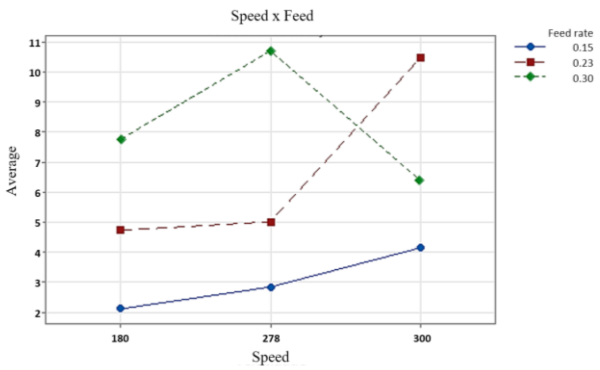

(a)

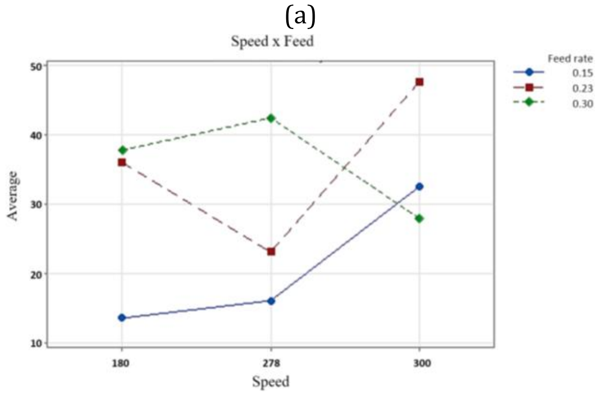

(b)

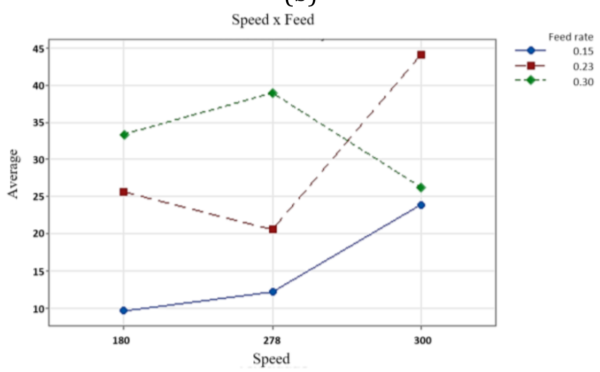

(c)

Fig. 6. Interaction plots of parameters for C45 +SR samples. (a) R_a, (b) R_t and (c) R_z.

For the R_z roughness parameter, it can be observed that transitioning from a cutting speed of 278 $m.min^{-1}$ to 300 $m.min^{-1}$ has a more significant impact than the change from 180 $m.min^{-1}$ to 278 $m.min^{-1}$. Regarding the feed rate, the change from 0.15 $mm.rev^{-1}$ to 0.23 $mm.rev^{-1}$ results in a marked effect on the response variable, unlike the change from 0.23 $mm.rev^{-1}$ to 0.30 $mm.rev^{-1}$. Overall, the behaviour of the feed rate follows a very similar pattern to that observed in the effects plots for R_a and R_t, supporting the discussions by Revel [32] and Ribeiro Filho [33] who assert that, among cutting conditions, the feed rate is the most influential parameter.

Fig. 6 illustrates a significant interaction between the feeds of 0.23 $mm.rev^{-1}$ and 0.30 $mm.rev^{-1}$ across all three roughness parameters. This effect is indicated by the crossing lines corresponding to these values, suggesting that the effect of varying the cutting speed level on the roughness response depends on the feed level. Hence, there is an interaction between the cutting speed and feed factors. Similar interaction trends were reported in the statistical studies conducted by Toledo [34] and Devor [35].

3.4. ANOVA analysis for experiments with normalized C45 steel

Fig. 7 illustrates the Pareto charts, providing a visual representation of the estimated individual effects of the independent variables on the different roughness parameters.

It can be observed that all the variables significantly impact the model for all roughness parameters, contributing substantially to the variation in the dependent variable, as none of them fall below the minimum significance threshold of 1980. For the R_a parameter, it is noted that the cutting feed variable had the most significant impact on the variation of the dependent variable, followed by the cutting speed, and finally by the interaction between the cutting speed and feed. Equivalent results were observed in research conducted by Biasibetti [14] and Filho [30].

For the R_t and R_z parameters, the cutting speed variable emerged as the main significant contributor to the variation of the dependent variable, followed by the feed, and finally, by the interaction between the cutting speed and feed. This behaviour contrasts with that observed for the R_a parameter, where feed showed the greatest significant impact on the variation of the dependent variable, followed by the cutting speed.

In the residual plots (Fig. 8), it can be observed that the residuals show a distribution close to normality, as indicated by the proximity of the points to the line, with a few outliers in the normal probability plot. The histograms of the residuals also approach normality, showing a distribution with a slight left skew. Such findings align with the statistical concepts discussed by Walpole [31], indicating that residuals displaying an approximately normal distribution with slight skewness validate the suitability of the model assumptions and support the robustness of the regression analysis.

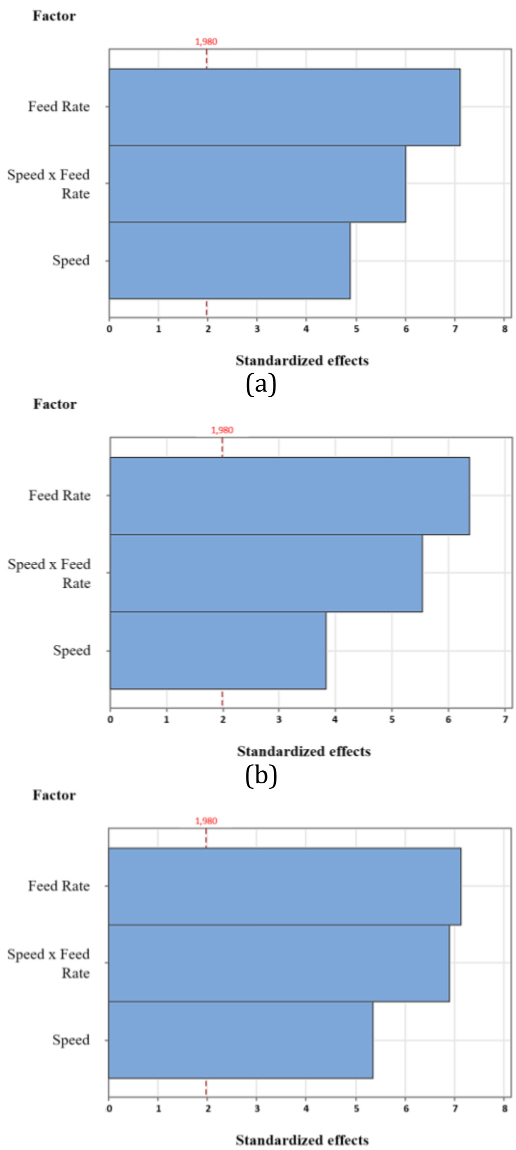

Fig. 7. Pareto Charts showing Standardized Effects of the Parameters for C45 +N Samples, α = 0.05. (a) R_a, (b) R_t and (c) R_z.

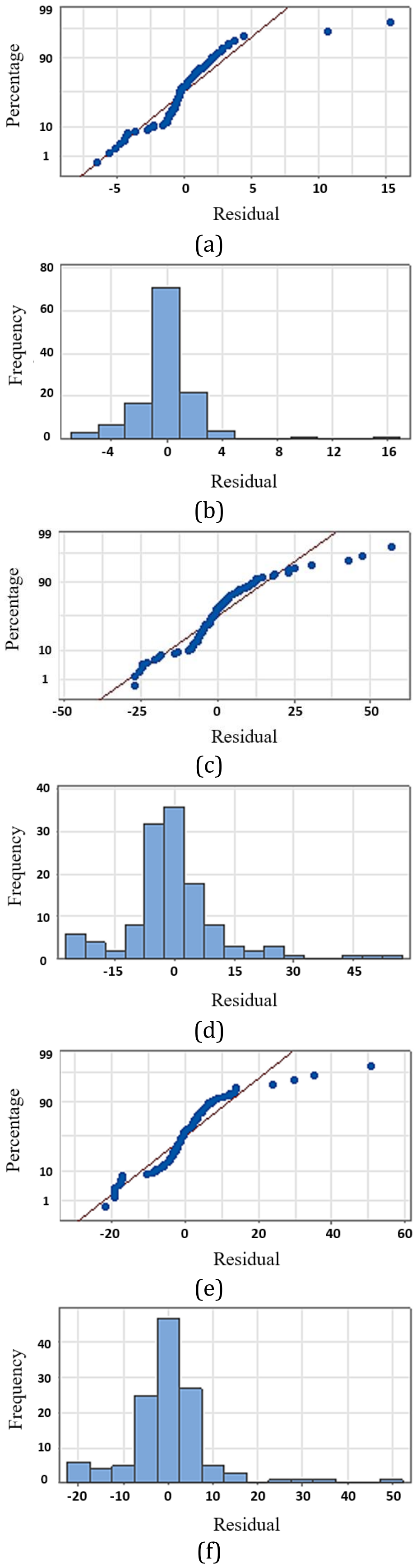

Fig. 8. Residual Plots of Parameters for C45 +N Samples: (a) R_a normal probability, (b) R_a histogram, (c) R_t normal probability, (d) R_t histogram, (e) R_z normal probability and (f) R_z histogram.

Fig. 9 presents the main effects plots for the R_a, R_t and R_z parameters. For the R_a parameter, a reduction in roughness is observed when advancing from 0.15 mm.rev^{-1} to 0.23 mm.rev^{-1}, while transitioning from 0.25 mm.rev^{-1} to 0.30 mm.rev^{-1} results in a significant increase in roughness.

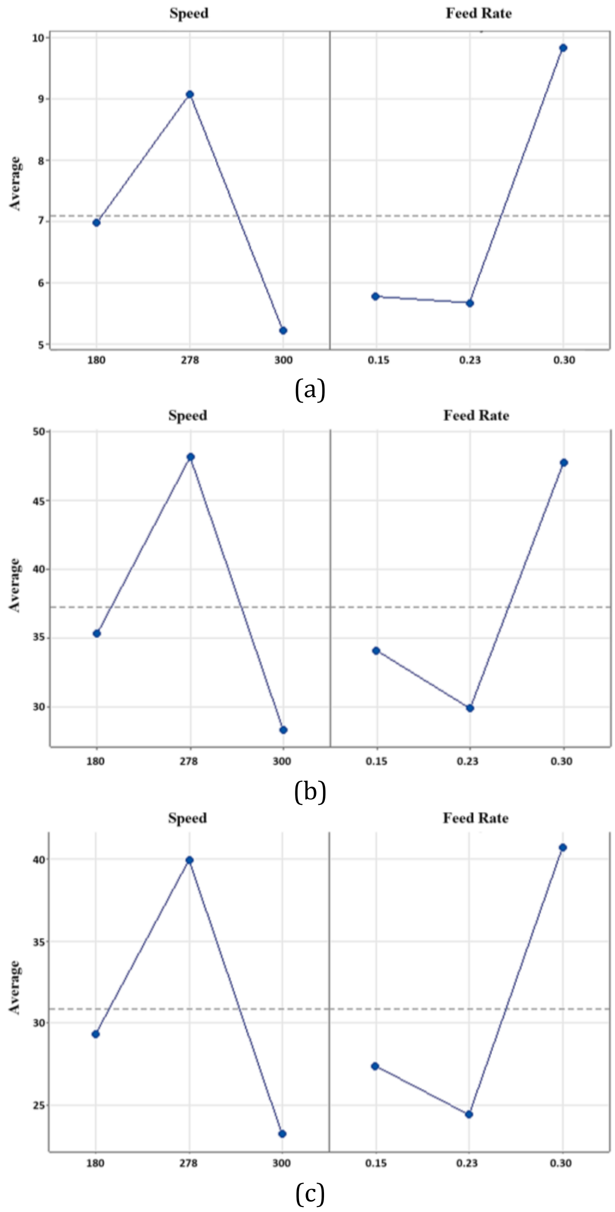

Fig. 9. Main effects plots of parameters for C45 +N samples. a) R_a, b) R_t and c) R_z.

Regarding the cutting speed, there is a noticeable increase in roughness when changing the cutting speed from 180 m.min^{-1} to 278 m.min^{-1}, followed by a significant decrease when the cutting speed changes from 278 m.min^{-1} to 300 m.min^{-1}. The behaviours observed for the samples with the +N heat treatment differ from those of the +SR treatment, which showed more linear graphs. An inverse behaviour in roughness is observed for the cutting speed and feed rate compared to the effect plots of the R_t parameter for the +SR steel. An increase in Rt is noted when the cutting speed is changed from 180 m.min-1 to 278 m.min-1, followed by a sharp decrease in roughness when the cutting speed is increased from 278 m.min-1 to 300 m.min-1.

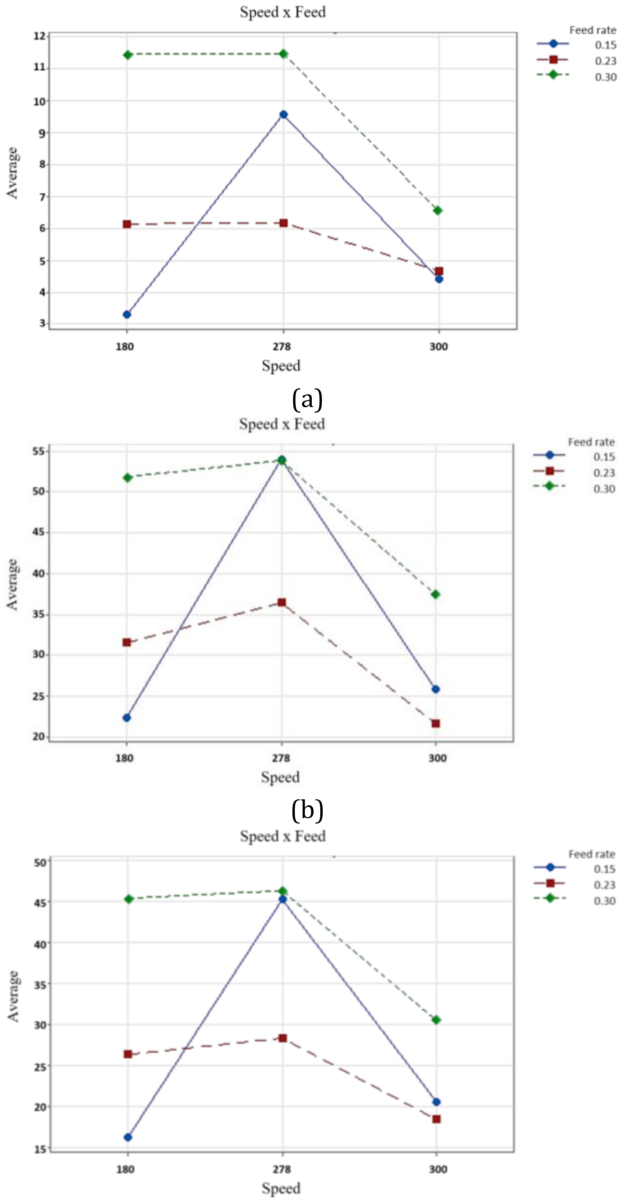

(a) (b) (c)

Fig. 10. Interaction plots of parameters for C45 +N samples. a) R_a, b) R_t and c) R_z.

For the feed rate, a reduction in roughness is observed when the feed rate is changed from 0.15 mm.rev-1 to 0.23 mm.rev-1, followed by a considerable increase in roughness when the feed rate is modified from 0.23 mm.rev-1 to 0.30 mm/rev. For the main effects plot of the Rz parameter, an inverse pattern of roughness behaviour is observed compared to the +SR steel R_z parameter effect plots, with a behaviour similar to the main effects plot of R_t roughness for the +N steel. An increase in R_z is observed when the cutting speed is changed from 180 m.min-1 to 278 m.min-1, followed by a sharp decrease in roughness when the cutting speed is increased from 278 m.min-1 to 300 m.min-1. Regarding the feed rate, a reduction in roughness is observed when the feed rate is changed from 0.15 mm.rev-1 to 0.23 mm.rev-1, followed by a considerable increase in roughness when the feed rate is modified from 0.23 mm.rev-1 to 0.30 mm/rev.

In Fig. 10, for the R_a parameter, a significant interaction is noted only between the feed rates of 0.15 mm.rev-1 and 0.23 mm.rev-1. This is clearly observed by the crossing lines corresponding to these two feed values. This dynamic contrasts with the interaction plot of R_a roughness for +SR steel, which revealed a significant interaction at feed rates of 0.23 mm.rev-1 and 0.30 mm.rev-1. For the R_t parameter, a significant interaction is observed among all three feed rates, indicating a strong correlation between these factors. This phenomenon can be clearly observed by the crossing lines associated with these three feed values. Comparable significant interactions between cutting parameters in the helical milling process were also identified by Toledo [34], supporting the trends observed in the present study. This type of interaction between the feed rates was also observed in the interaction plot of R_t in +SR steel. For the R_z roughness parameter, a significant interaction is noted between the feed rates of 0.15 mm.rev-1 and 0.23 mm.rev-1, as seen by the crossing lines associated with these feed values. When comparing the interaction plot of the same R_z roughness parameter in +SR steel, it can be observed that the significant interaction was between the feed rates of 0.23 mm.rev-1 and 0.30 mm.rev-1. Furthermore, through graphical analysis, it can be observed how the influence of the cutting speed on the response varies at different feed rates. Considering the feed rate fixed at 0.15 mm.rev-1 and the cutting speed that changed from 180 m.min-1 to 278 m.min-1, the R_z roughness increased by an average of about 30 units, revealing a notably significant result.

3.5. Analysis of chip formation in the dry internal turning process of C45 steel

The chips were analysed and classified according to the NBR ISO 3685 standard [20], considering the shape and type of chips formed. In both conditions, C45 +SR and C45 +N, the predominant shape was in the form of fragmented chips in flakes or pieces. This morphology is similar to disconnected arc chips (comma) and fragmented chips, categorized as chip forms 6.2 and 7, respectively.

The production of short or fragmented chips is a positive aspect of machinability, as it offers many advantages, such as a low specific volume, which favours process automation, ease of removal, and reduced risk of accidents for machine operators. For a more in-depth analysis of the chip characteristics, the cutting speed fixation metric with varying feed rates was used. According to Arbizu and Perez [28], Kumar and Chauran [29] and Barzani [23], the cutting parameters that most influence chip formation are the feed rate, followed by the cutting depth.

Fig. 11 shows the morphology of the chips generated for different feed rates and cutting speeds, characterized according to the classification established by the ABNT NBR ISO 3685 standard [20]. In experiments 1 (0.15-180), 2 (0.15-278), and 5 (0.23-278), all planned machining passes were carried out smoothly, maintaining a consistent morphology of fragmented chips throughout the process.

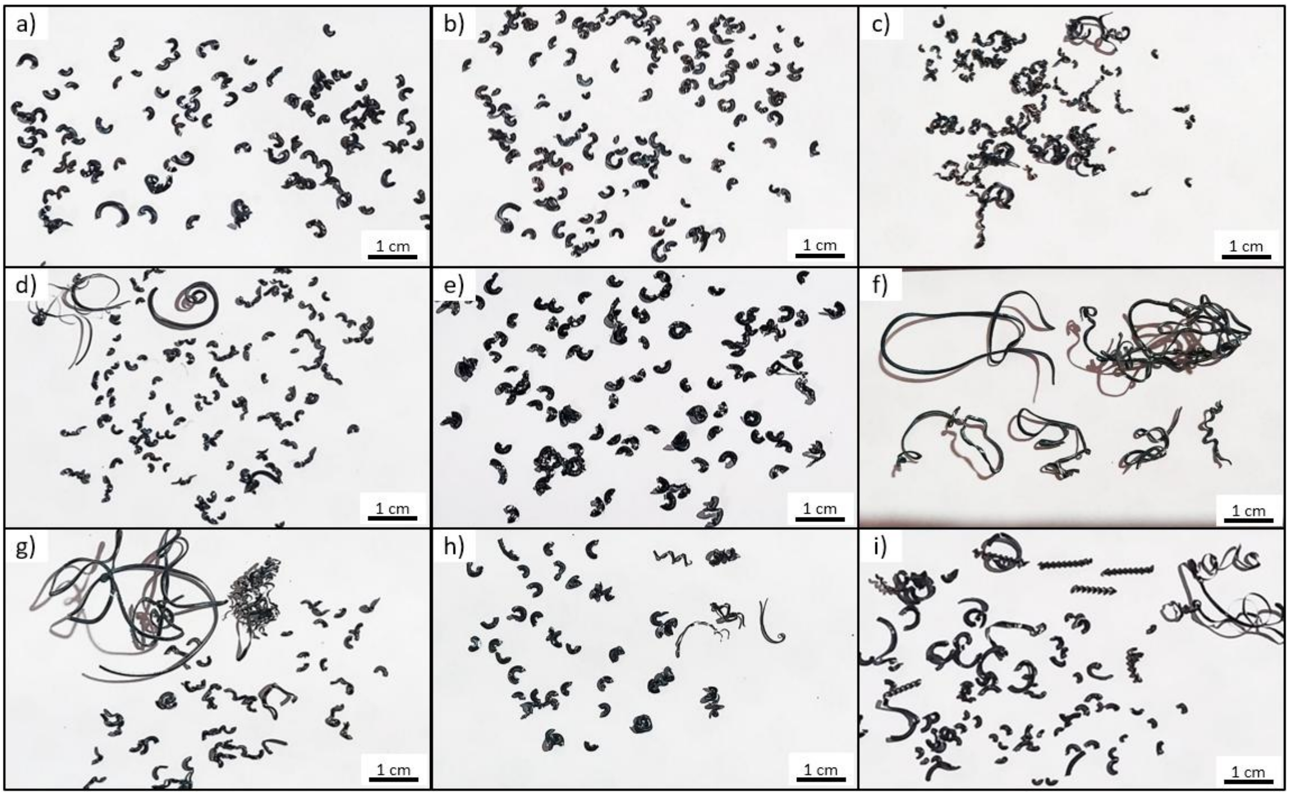

Fig. 11. Chip Morphology from Experiments with DIN C45 +SR Steel: a) 0.15-180, b) 0.15-278, C) 0.15-300, d) 0.23-180, e) 0.23-278, f) 0.23-300, g) 0.30-180, h) 0.30-278 and i) 0.30-300.

The morphology of the chips in experiments 4 (0.23-180), 6 (0.23-300), 7 (0.30-180), 8 (0.30-278), and 9 (0.30-300) showed short chips prone to entanglement, short ribbons, and entangled short ribbons. These types of chips were associated with the highest feeds within their groups, considering a constant cutting speed. Despite having a low feed experiment 3 (0.15-300) also showed impaired chip morphology. It is suggested that the combination with the highest cutting speed might have contributed to a potential increase in turning temperature and cutting force, although these factors were not addressed in this study. This behaviour aligns with the observations of Singh [36], who reported that an increase in cutting speed reduces the degree of chip segmentation, resulting in the formation of smaller, discontinuous chips, a condition favourable for high-speed machining. These findings were established through a detailed study of chip morphology in the turning of AISI 4340 steel.

3.6. Analysis of chips for normalized C45 steel (+N)

As shown in Fig. 12, the morphology of chips generated in experiments 1 (0.15-180), 3 (0.15-300), 4 (0.23-180), 6 (0.23-300), and 7 (0.30-180) did not show morphological differences among them, maintaining a shape consistent with fragmented chips. The chip morphology from experiments 2 (0.15-278), 5 (0.23-278), and 8 (0.30-278)3685 generally showed chips in fragmented, disconnected, and comma-like shapes. However, a special cause was identified in experiment 2 (0.15-278), which resulted in short, tangled ribbon-type chips during the second machining pass. The special cause was attributed to the wear of the insert seat in the tool holder. After correcting the anomaly, the experiment continued smoothly, maintaining the fragmented chip type observed in the other two experiments of this group.

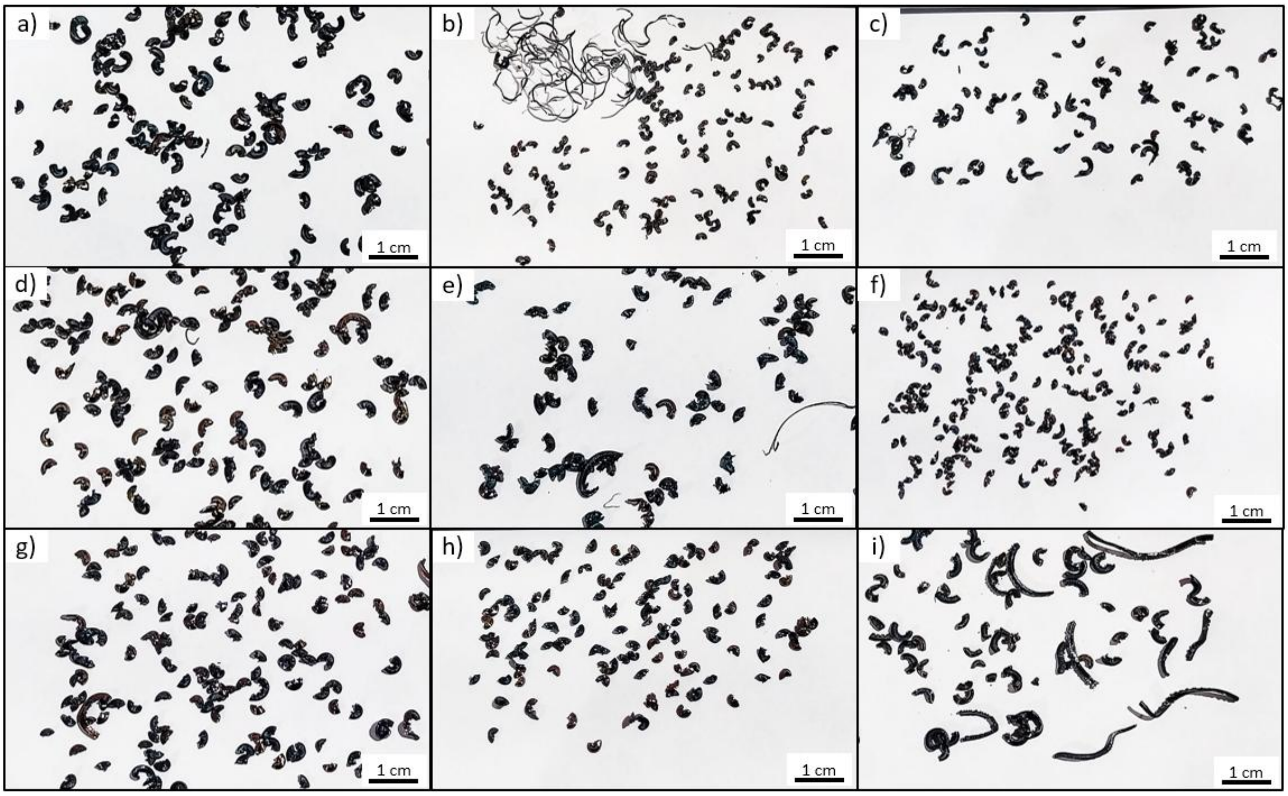

Fig. 12. Chip Morphology from Experiments with DIN C45 +N Steel: a) 0.15-180, b) 0.15-278, C) 0.15-300, d) 0.23-180, e) 0.23-278, f) 0.23-300, g) 0.30-180, h) 0.30-278 and i) 0.30-300.

Comparing the chip characteristics produced in experiments with C45 steel with stress relief and normalized, it is generally observed that the +N state showed fewer issues with chip formation. In these experiments, the chip morphology remained predominantly fragmented. In contrast, most of the experiments with C45 +SR encountered difficulties in chip formation, resulting in various morphologies such as short chips prone to tangling, short ribbon chips, and tangled short ribbons. In the experiments conducted with C45 +N steel, greater stability in chip formation was observed, with less variation in chip morphology. This consistency can be attributed to the material's microstructure, which significantly influences machining performance, as also highlighted in the studies of Strafford [37] and Singh [38]. The normalized structure of the material undergoes a heating process to austenitization temperature for sufficient time for complete normalization, followed by cooling to ambient temperature. This process results in mechanical properties and a structure that provides more favourable conditions for machining, as demonstrated in this study, regardless of the various cutting parameter configurations used in the experiments.

4. CONCLUSION

The statistical study showed that for the three R_a, R_z and R_t roughness parameters, all models, including the individual factors and interactions, were statistically significant at a 5 % level (P-value < 0.05). This result suggests that at least one of the independent variables analysed has a significant effect on the dependent variable. An observable increase in roughness was detected as the feed rate was amplified.. Experiments with the lowest feed rates, 0.15 mm.rev^{-1} and 0.23 mm.rev^{-1}, showed the optimal results for the C45 steel in both thermal treatments evaluated. Regarding the chips, for the stress relief steel samples, the combinations that demonstrated ideal chip conditions were those with the lowest feed rates, specifically the feed and cutting speed combinations: 0.15-180, 0.15-278, and 0.23-278. For the steel with the normalization treatment, almost all the cutting parameters showed the best performance, covering both lower and higher feed and cutting speed combinations, except for the 0.30-300 parameter, which showed the poorest performance. A comparison of the characteristics of chips produced in experiments with C45 steel in both stress-relieved and normalized states reveals that the normalized state generally exhibited fewer issues related to chip formation. In experiments with the normalized state, the chip morphology remained predominantly fragmented. In contrast, a majority of experiments with stress-relieved C45 steel showed poorer chip formation results, resulting in range of morphologies, including short chips prone to entangling, short ribbon-like chips, and entangled short ribbons. From an industrial perspective, the findings of this study provide significant practical contributions to C45 steel turning operations. It was observed that normalized C45 steel exhibits superior machinability compared with stress-relieved steel, particularly in terms of chip control and surface finish quality. Furthermore, lower feed rates (0.15–0.23 mm·rev^{-1}) proved to be more suitable for achieving smoother surfaces and controlled chip formation, thereby contributing to reduced tool wear and enhanced process stability. The application of the identified relationships between cutting parameters and machinability outcomes can, significantly, reduce the time required for empirical testing in production environments. In parallel, the integration of experimental design and statistical analysis methods has demonstrated efficacy in improving process reliability, enabling a more precise and rational selection of cutting parameters. Overall, the findings of this work highlight the potential for cost reduction and productivity improvement, resulting from the optimized definition of machining parameters, the reduction of setup time, and the decreased dependence on empirical, trial-and-error approaches in turning operations.

Acknowledgments

The authors would like to acknowledge the Graduate Program in Materials Engineering of the Federal Center for Technological Education of Minas Gerais. This study was financed in part by the Coordenação de Aperfeiçoamento de Pessoal de Nível Superior - Brazil (CAPES) - Finance Code 001.

REFERENCES

[1] N. Puneeth Kumar, and A. S. Srikantappa, "Temperature and Tool Wear Analysis on Machining of Two Different Composition of C45 Steel," *International Journal of Engineering Research & Technology,* vol. 11, no. 08, pp. 208, 2022, doi: 10.17577/IJERTV11IS080126.

[2] B. Bialobrzeska, R. Dziurka, A. Żak, and P. Bala, "The influence of austenitization temperature on phase transformations of supercooled austenite in low-alloy steels with high resistance to abrasion wear," *Archives of Civil and Mechanical Engineering,* vol. 18, no. 2, pp. 413-429, 2018, doi: 10.1016/j.acme.2017.09.004.

[3] F. G. Caballero, C. Capdevila and C. G. Andrés, "Modelling of Kinetics of Austenite Formation in Steels with Different Initial Microstructures," *ISIJ International,* vol. 41, no. 10, pp. 1093-1102, 2001, doi: 10.2355/isijinternational.41.1093.

[4] E. C. T. Ba, P. S. Martins and M. R. Dumont, "Statistical study of surface texture and chip formation during turning of AISI 1020 steel: Emphasis on parameters Rsk, Rku, and Rk family and on the chip thickness ratio," *The International Journal of Advanced Manufacturing Technology,* vol. 121, pp. 8257-8283, 2022, doi: 10.1007/s00170-022-09919-1.

[5] A. P. Paiva, J. R. Ferreira and P. P. Balestrassi, "A multivariate hybrid approach applied to AISI 52100 hardened steel turning optimization," *Journal of Materials Processing Technology,* vol. 189, no. 1-3, pp. 26-35, 2007, doi: 10.1016/j.jmatprotec.2006.12.047.

[6] N. Mandal, B. Doloi and B. Mondal, "Development of flank wear prediction model of Zirconia Toughened Alumina (ZTA) cutting tool using response surface methodology," *International Journal of Refractory Metals and Hard Materials,* vol. 29, no. 2, pp. 273-280, 2011, doi: 10.1016/j.ijrmhm.2010.12.001.

[7] T. Ozel, Y. Karpat, L. Figueira and J. P. Davim, "Modelling of surface finish and tool flank wear in turning of AISI D2 steel with ceramic wiper inserts," *Journal of Materials Processing Technology,* vol. 189, no. 1-3, pp. 192-198, 2007, doi: 10.1016/j.jmatprotec.2007.01.021.

[8] W. Grzesik, "Wear development on wiper Al2O3–TiC mixed ceramic tools in hard machining of high strength steel," *Wear,* vol. 266, no. 9-10, pp. 1021-1028, 2009, doi: 10.1016/j.wear.2009.02.010.

[9] V. N. Gaitonde, S. R. Karnik, L. Figueira and J. P. Davim, "Machinability investigations in hard turning of AISI D2 cold work tool steel with conventional and wiper ceramic inserts," *International Journal of Refractory Metals and Hard Materials,* vol. 27, no. 4, pp. 754-763, 2009, doi: 10.1016/j.ijrmhm.2008.12.007.

[10] M. Soori, F. K. G. Jough, R. Dastres and B. Arezoo, "Sustainable CNC machining operations, a review," *Sustainable Operations and Computers,* vol. 5, pp. 73-87, 2024, doi: 10.1016/j.susoc.2024.01.001.

[11] P. S. Bilga, S. Singh and R. Kumar, "Optimization of energy consumption response parameters for turning operation using Taguchi method," *Journal of Cleaner Production,* vol. 137, pp. 1406-1417, 2016, doi: 10.1016/j.jclepro.2016.07.220.

[12] Z. Liao, J. M. Schoop, J. Saelzer, B. Bergmann, P. C. Priarone, A. Splettstößer, V. M. Bedekar, F. Zanger and Y. Kaynak, "Review of current best-practices in machinability evaluation and understanding for improving machining performance," *CIRP Journal of Manufacturing Science and Technology,* vol. 50, pp. 151-184, 2024, doi: 10.1016/j.cirpj.2024.02.008.

[13] S. N. Grigoriev, S. V. Fedorov and K. Hamdy, "Materials, properties, manufacturing methods and cutting performance of innovative ceramic cutting tools – a review," *Manufacturing Review,* vol. 6, 2019, Art. no. 19, doi: 10.1051/mfreview/2019016.

[14] G. R. S. Biasibetti, R. M. Nunes, L. C. C. Cavaler and A. S. Rocha, "Surface roughness analyses of 0.45%c (SAE 1045) steel bars after turning," *Matéria,* vol. 1, 2019, doi: 10.1590/S1517-707620190001.0630.

[15] O. Keblouti, L. Boulanouar, M. W. Azizi and M. A. Yallese, "Modeling and multi-objective optimization of surface roughness and productivity in," *International Journal of Industrial Engineering Computations,* vol. 8, pp. 71-78, 2017, doi: 10.5267/j.ijiec.2016.7.002.

[16] Steels for quenching and temperin - Part 2: techical delivery conditions for non alloy steels, DIN EN 10083-2, Deutsches Institut für Normung, 2006.

[17] E. S. Gadelmawla, M. M. Koura, T. M. A. Maksoud, I. M. Elewa and H. H. Soliman, "Roughness parameters," *Journal Of Materials Processing Technology,* vol. 123, no. 1, pp. 133-145, 2002, doi: 10.1016/S0924-0136(02)00060-2.

[18] J. Das and B. Linke, "Evaluation and systematic selection of significant multi-scale surface roughness parameters (SRPs) as process monitoring index," *Journal of Materials Processing Technology,* vol. 244, pp. 157-165, 2017, doi: 10.1016/j.jmatprotec.2017.01.017.

[19] Standard Test Methods and Definitions for Mechanical Testing of Steel Products, ASTM A370, ASTM International, 2023.

[20] Ensaio de vida da ferramenta de ponta única para torneamento, ABNT NBR ISO 3685, Associação Brasileira de Normas Técnicas, 2017.

[21] D. C. Montgomery and G. C. Runger, *Applied Statistics and Probability for Engineers*, 5th ed. John Wiley & Sons, Inc., 2011.

[22] D. C. Montgomery, *Design and Analysis of Experiments,* John Wiley & Sons, 2017.

[23] M. M. Barzani, E. Zalnezhad, A. A. D. Sarhan, S. Farahany and S. Ramesh, "Fuzzy logic based model for predicting surface roughness of machined Al-Si-Cu-Fe die casting alloy using different additives-turning," *Measurement,* vol. 61, pp. 150-161, 2015, doi: 10.1016/j.measurement.2014.10.003.

[24] D. E. Coleman and D. C. Montgomery, "A systematic approach to planning for a designed industrial experimente," *Technometrics,* vol. 35, no. 1, pp. 1-12, 1993, doi: 10.1080/00401706.1993.10484984.

[25] H. Zhu, K. Xu, S. Qin, F. Xiao and B. Liao, "Effect of heat treatment on microstructure and properties of 1045 steel modified with (NbTi)C nanoparticles," *Materials Science and Engineering: A,* vol. 728, pp. 175-182, 2018, doi: 10.1016/j.msea.2018.05.019.

[26] H. K. D. H. Bhadeshia and R. W. K. Honeycombe, *Steels: Microstructure and properties*, 4th ed., Oxford: Butterworth-Heinemann, 2017.

[27] S. Singh, S. Samir, K. Kumar and S. Thapa, "Effect of heat treatment processes on the mechanical properties of AISI 1045 steel.," *Materials today: proceedings,* vol. 45, no. 6, pp. 5097-5101, 2021, doi: 10.1016/j.matpr.2021.01.590.

[28] I. P. Arbizu and C. J. L. Luis Pérez, "Surface roughness prediction by factorial design of experiments in turning processes," *Journal of Materials Processing Technology,* Vols. 143-144, pp. 390-396, 2003, doi: 10.1016/S0924-0136(03)00407-2.

[29] R. Kumar and S. Chauran, " Study on surface roughness measurement for turning of Al7075/10/SiCp and Al7075 hybrid composites by using response surface methodology (RSM) and artificial neural networking (ANN)," *Measurement,* vol. 65, pp. 166-180, 2015, doi: 10.1016/j.measurement.2015.01.003.

[30] A. F. L. Filho, N. W. Paschoalinoto, J. A. G. Ferrer, O. L. Padovan, C. O. Kenvyn and J. R. Camargo, "Application of a factorial planning for the prediction of surface finishing of the milling process of alloy Ti-6AL-4V," *Brazilian Journal of Development,* vol. 7, no. 2, p. 20294–20310, 2021, doi: 10.34117/bjdv7n2-598.

[31] R. E. Walpole, R. H. Myers, S. L. Myers and K. Ye, *Probability & Statistics for Engineers & Scientists*, 9th ed., Boston: Pearson, 2011.

[32] P. Revel, N. Jouini, G. Thoquenne and F. Lefebvre, "High precision hard turning of AISI 52100 bearing steel," *Precision Engineering,* vol. 43, pp. 24-33, 2016, doi: 10.1016/j.precisioneng.2015.06.006.

[33] S. L. M. Ribeiro Filho, C. H. Lauro, A. H. S. Bueno and L. C. Brandrão, "Influence cutting parameters on the surface quality and corrosion behavior of Ti-6Al-4V alloy in synthetic body environment (SBF) using Response Surface Method," *Measurement,* vol. 88, pp. 223-237, 2016, doi: 10.1016/j.measurement.2016.03.047.

[34] J. V. R. Toledo, T. F. Pires, R. B. D. Pereira and J. R. Ferreira, "A multi-objective robust evolutionary optimization approach applied to the multivariate helical milling process of super duplex steel," *Applied Soft Computing,* vol. 147, p. 110811, 2023, doi: 10.1016/j.asoc.2023.110811.

[35] R. E. Devor, T. H. Chang and J. W. Sutherland, Statistical quality design and control: contemporary concepts and methods, 2nd ed., New York: Prentiss-Hall, 2007.

[36] B. K. Singh, H. Roy, B. Mondal, S. S. Roy and N. Mandal, "Measurement of chip morphology and multi criteria optimization of turning parameters for machining of AISI 4340 steel using Y-ZTA cutting insert," *Measurement,* vol. 142, pp. 181-194, 2019, doi: 10.1016/j.measurement.2019.04.064.

[37] K. N. Strafford and J. Audy, "Indirect monitoring of machinability in carbon steels by measurement of cutting forces," *Journal of Materials Processing Technology,* vol. 67, no. 1-3, pp. 150-156, 1997, doi: 10.1016/S0924-0136(96)02835-X.

[38] S. B. Singh, A. K. Chakrabarti and A. B. Chattopadhyay, "A study of the effect of inclusion content of the machinability and wear characteristics of 0.24% carbon steels," *Journal of Materials Processing Technology,* vol. 66, no. 1-3, pp. 90-96, 1997, doi: 10.1016/S0924-0136(96)02500-9.